

Synthesis, Characterization, and Photophysical Properties of a Series of Supramolecular Mixed-Valence Compounds

Brian W. Pfennig,* Virginia A. Fritchman, and Katie A. Hayman

Department of Chemistry, Vassar College, 124 Raymond Avenue, Poughkeepsie, New York 12604

Received June 27, 2000

The synthesis and characterization of 10 cyano-bridged trinuclear mixed-valence compounds of the form $[(\text{NH}_3)_5\text{M}-\text{NC}-\text{Fe}^{\text{II}}(\text{CN})_4-\text{CN}-\text{M}'(\text{NH}_3)_5]^{n+}$ ($\text{M} = \text{Ru}^{\text{III}}, \text{Os}^{\text{III}}, \text{Cr}^{\text{III}}, \text{or Pt}^{\text{IV}}; n = 2, 3, \text{ or } 4$) is reported. The electronic spectra of these supramolecular compounds exhibit a single intervalent (IT) absorption band for each nondegenerate $\text{Fe} \rightarrow \text{M}/\text{M}'$ transition. The redox potential of the $\text{Fe}(\text{II})$ center is shifted more positive with the addition of each coordinated metal complex, while the redox potentials of the pendant metals vary only slightly from their dinuclear counterparts. As a result, the $\text{Fe} \rightarrow \text{M}$ IT bands are blue-shifted from those in the corresponding dinuclear mixed-valence compounds. The energies of these IT bands show a linear correlation with the ground-state thermodynamic driving force, as predicted by classical electron transfer theory. Estimates of the degree of electronic coupling (H_{ab}) between the metal centers using a theoretical analysis of the IT band shapes indicate that most of these values are similar to those for the corresponding dinuclear species. Notable exceptions occur for the $\text{Fe} \rightarrow \text{M}$ IT transitions in $\text{Os}-\text{Fe}-\text{M}$ ($\text{M} = \text{Cr}$ or Pt). The enhanced electronic coupling in these two species can be explained as a result of excited state mixing between electron transfer and/or ligand-based charge transfer states and an intensity-borrowing mechanism. Additionally, the possibility of electronic coupling between the remote metal centers in the $\text{Ru}-\text{Fe}-\text{Ru}$ species is discussed in order to explain the observation of two closely spaced redox waves for the degenerate $\text{Ru}(\text{III})$ acceptors.

Introduction

Mixed-valence (MV) compounds are species which contain an electronically coupled donor (D)/acceptor (A) pair within the same molecular unit, either as an outer-sphere ion pair, directly bonded to each other, or connected by a ligand bridge.¹ One of the earliest and best known examples is that of Prussian blue, a three-dimensional polymeric array of C-bound $\text{Fe}(\text{II})$ and N-bound $\text{Fe}(\text{III})$ units linked by bridging cyanides, which has been used as a pigment for several centuries.² In the late 1960s, Hush predicted that MV compounds should exhibit a low-energy intervalent (IT) band in their electronic absorption spectra as a result of this D/A coupling.³ For valence-localized MV compounds, the theory predicted that the energy of the IT band (E_{op}) should equal the sum of the reorganization energy (λ) and the ground-state free energy difference (ΔG°), according to eq 1. Furthermore, the magnitude of the electronic coupling

$$E_{\text{op}} = \lambda + \Delta G^\circ \quad (1)$$

(H_{ab}) can be inferred from the oscillator strength of the IT absorption band, according to eq 2, where ϵ_{max} ($\text{M}^{-1} \text{cm}^{-1}$) is

$$H_{\text{ab}} = \frac{0.0206 \left(\epsilon_{\text{max}} \nu_{\text{max}} \frac{\Delta \nu_{1/2}}{g} \right)^{1/2}}{r_{\text{ab}}} \quad (2)$$

the molar absorptivity of the IT band at its maximum value, $\Delta \nu_{1/2}$ (cm^{-1}) is the full width at half-maximum, ν_{max} (cm^{-1}) is the frequency of the IT band, g is the degeneracy of the

transition, and r_{ab} (\AA) is the distance the electron must traverse between D and A, commonly estimated as the crystallographic distance between the metal centers. Beginning in the late 1960s with the synthesis of the Creutz–Taube ion,⁴ $[(\text{NH}_3)_5\text{Ru}-\text{pz}-\text{Ru}(\text{NH}_3)_5]^{5+}$ ($\text{pz} = \text{pyrazine}$), the development of designed mixed-valence compounds allowed for a systematic investigation of the validity of eqs 1 and 2 in describing the properties of covalently linked D/A compounds. Indeed, the Creutz–Taube ion sparked a decade-long controversy about whether the two Ru oxidation states were better described as valence localized (2+ and 3+) or delocalized (2.5+ and 2.5+). Mixed-valence compounds have therefore played a crucial historical role in the exploration of electron transfer theory.

Mixed-valence compounds continue to be an important experimental tool for addressing contemporary issues in electron transfer research.⁵ Recent emphasis in this field has shifted away from simple dinuclear MV species and focused instead on multinuclear supramolecular species. These compounds are constructed from discrete molecular units which largely retain their individual characteristics, but which also possess properties unique to the larger structure as a whole. Multinuclear MV compounds have been suggested in the design of electrochromic devices, solar energy conversion catalysts, photoinduced magnetic memory devices, chemical sensors, nanoscale switches with ultrafast write times, and molecular-scale rectifiers.⁶ Despite the diversity of these potential applications, relatively little is known about how the properties of electron transfer between a

* To whom correspondence should be addressed.

(1) Creutz, C. *Prog. Inorg. Chem.* **1989**, *30*, 1–73.

(2) Woodward, J. *Philos. Trans. R. Soc. London* **1724**, *33*, 15.

(3) Hush, N. S. *Prog. Inorg. Chem.* **1967**, *8*, 391–443.

(4) Creutz, C.; Taube, H. *J. Am. Chem. Soc.* **1969**, *91*, 3988.

(5) Barbara, P. F.; Meyer, T. J.; Ratner, M. A. *J. Phys. Chem.* **1996**, *100*, 13148–13168.

(6) Ferretti, A.; Lami, A.; Ondrechen, M. J.; Villani, G. *J. Phys. Chem.* **1995**, *99*, 10484–10491 and references therein.

single donor and acceptor are influenced by their inclusion into larger supramolecular assemblies.

One physical property of particular importance in the development of useful molecular devices is the degree of electronic coupling, since this is a critical parameter in dictating the rate of intramolecular electron transfer. Electronic communication between metal centers is especially important in the design of nanoscale electronic devices where molecular wires will be required to conduct electrical charge over long distances. It is also relevant in macromolecular systems of biological interest. The magnitude of the electronic coupling is defined by H_{ab} , the matrix element $\langle \Phi_D | H | \Phi_A \rangle$, where H is the Hamiltonian derived from first-order perturbation theory and Φ_D and Φ_A are the diabatic electronic wave functions for the ground and excited electron transfer states, respectively.⁷ This electronic interaction manifests itself in the oscillator strength of the IT absorption band, shifts in the electrochemical potentials of the metals in the MV complex which result from a thermodynamic stabilization of the ground state, the rates of intramolecular electron transfer, and physical properties of the ligand bridge.⁸ Several theories have been postulated for how the electronic interaction can occur over long distances in supramolecular or biological molecules. The most common of these models involves a superexchange mechanism, in which the D and A electron transfer states are coupled to each other through mixing of these states with higher lying excited states involving the bridging ligand (e.g., MLCT or LMCT excited states).^{7,9} A vibronic coupling mechanism has also been proposed, where the electronic and nuclear coordinates are entangled or coupled with each other such that the equilibrium nuclear configuration varies as a function of the electronic charge delocalized onto the bridging ligand.¹⁰ This model has been used to explain the intriguing red shifts of $\nu(\text{CN})$ in cyano-bridged MV compounds, whose energies are roughly correlated with the intensity of the IT band.⁸ It has also led to the development of a vibronic selection rule which can cause the superexchange contribution to H_{ab} to disappear in certain trinuclear D/A compounds.¹¹

Cyano-bridged mixed-valence compounds are particularly attractive systems for an investigation of electronic coupling in supramolecular D/A compounds because the strong π -acidic nature of the cyanide ligand facilitates overlap of the $d\pi$ orbitals of the donor and acceptor metals with the perpendicular π^* molecular orbitals of the ligand bridge.⁹ A second advantage is that the MLCT, LMCT, and LF transitions which result from the strong ligand field nature of the cyanide ligand typically appear at higher energies than the IT band, thus preventing its obscuration.¹² The strong $\nu(\text{CN})$ stretches which occur in the IR can serve as markers of both the oxidation state and the coordination number of the central metal, as well as a measure of the degree of M–CN π back-bonding across the ligand bridge.^{13,14} For all of the above reasons, cyano-bridged mixed-

valence compounds have afforded experimentalists with a versatile family of complexes appropriate for a theoretical treatment of intramolecular electron transfer.

Experimental Section

Materials and Instrumentation. $\text{K}_4[\text{Fe}(\text{CN})_6] \cdot 3\text{H}_2\text{O}$ and $[\text{Os}(\text{NH}_3)_5(\text{OSO}_2\text{CF}_3)](\text{OSO}_2\text{CF}_3)_2$ were purchased from Aldrich, $[\text{Cr}(\text{NH}_3)_5\text{Cl}]\text{Cl}_2$ was obtained from Alfa, and $[\text{Ru}(\text{NH}_3)_5\text{Cl}]\text{Cl}_2$ was supplied by Strem. The pentaamminetrifluoromethanesulfonato metal complexes, $[\text{Pt}(\text{NH}_3)_5(\text{OSO}_2\text{CF}_3)](\text{OSO}_2\text{CF}_3)_3$, $[\text{Ru}(\text{NH}_3)_5(\text{OSO}_2\text{CF}_3)](\text{OSO}_2\text{CF}_3)_2$, and $[\text{Cr}(\text{NH}_3)_5(\text{OSO}_2\text{CF}_3)](\text{OSO}_2\text{CF}_3)_2$, were synthesized by combination of the appropriate pentaamminechloro species with trifluoromethanesulfonic acid (Aldrich) under an Ar atmosphere, according to their literature procedures.¹⁵ $[\text{Pt}(\text{NH}_3)_5\text{Cl}]\text{Cl}_3$ was prepared from $\text{K}_2[\text{PtCl}_6]$,^{15a} which in turn was synthesized by the addition of KCl to a concentrated aqueous solution of chloroplatinic acid.¹⁶ Bio-Gel P2 polyacrylamide gel was obtained from Bio-Rad.

Electronic absorption spectra (300–1100 nm) were obtained in aqueous solution in 1-cm plastic cuvettes by using a Hewlett-Packard 8453 diode array spectrophotometer. Infrared spectra (4000–400 cm^{-1}) were collected as KBr pellets as the average of eight scans by using a Perkin-Elmer 1600 Series FTIR with 2 cm^{-1} resolution. Cyclic voltammograms (CV) and differential pulse voltammograms (DPV) were obtained by using a standard three-electrode (C/Pt/SSE) configuration and a BAS CV-50W voltammetric analyzer. The supporting electrolyte was 0.2 M KNO_3 . For CV, scan rates of 10, 20, 50, 100, 200, and 500 mV were employed. For DPV, a scan rate of 4 mV/s, an amplitude of 10 mV, and a 50 ms pulse width were used. The metal:metal ratios of the cyano-bridged mixed-valence compounds (vide infra) and the concentrations of each metal in these solutions were determined by ICP atomic emission spectroscopy by using a SpectroFlame (Model D) ICP equipped with a Cross-Flow nebulizer and Smart Analyzer software. Standard curves for each metal were prepared from serial dilutions of two commercially available 100 ppm standards (Alfa Specpure precious metals plasma standard and EM trace metals standard no. 1). The wavelengths used in the analyses were 285.568, 259.940, 225.585, 265.945, and 373.003 nm for Cr, Fe, Os, Pt, and Ru, respectively. These wavelengths were chosen so as to minimize overlap from the nearby lines of the other metals present in the samples while maximizing the instrumental sensitivity. The results reported are the average of three consecutive analyses per sample. Owing to the difficulties involved in accurately weighing small amounts of high molecular weight compounds whose degree of hydration was not known, molar absorptivities were determined by obtaining UV/vis spectra of the pure compounds in aqueous solutions where the iron concentration had first been determined by ICP. The half-widths ($\Delta\nu_{1/2}$) of the electronic absorption bands were calculated by doubling the difference between the wavenumber at the absorption maximum and the wavenumber at half the height of the absorption maximum on the side of the band farthest from any potentially overlapping transitions. Unless otherwise stated, these bands were assumed to be symmetrical. For those spectra which contained two overlapping absorptions, the peaks were fit to Gaussian bands using the GRAMS 32 spectral analysis software package in order to obtain their half-widths and peak intensities.

Synthesis of the Dinuclear Mixed-Valence Compounds. $\text{K}[(\text{NH}_3)_5\text{Ru}^{\text{III}}\text{—NC—Fe}^{\text{II}}(\text{CN})_5]$,¹⁷ $\text{K}[(\text{NH}_3)_5\text{Os}^{\text{III}}\text{—NC—Fe}^{\text{II}}(\text{CN})_5]$,¹⁸ and $\text{K}[(\text{NH}_3)_5\text{Cr}^{\text{III}}\text{—NC—Fe}^{\text{II}}(\text{CN})_5]$ ¹⁸ were synthesized by slight modifications to their literature procedures, as follows: aqueous solutions (~15 mM)

- (7) Creutz, C.; Newton, M. D.; Sutin, N. *J. Photochem. Photobiol. A: Chem.* **1994**, *82*, 47–59.
 (8) Watzky, M. A.; Endicott, J. F.; Song, X.; Lei, Y.; Macatangay, A. *Inorg. Chem.* **1996**, *35*, 3463–3473 and references therein.
 (9) Scandola, F.; Argazzi, R.; Bignozzi, C. A.; Chiorboli, C.; Indelli, M. T.; Rampi, M. A. *Coord. Chem. Rev.* **1993**, *125*, 283–292.
 (10) Watzky, M. A.; Macatangay, A. V.; Van Camp, R. A.; Mazzetto, S. E.; Song, X.; Endicott, J. F.; Buranda, T. *J. Phys. Chem.* **1997**, *101*, 8441–8459.
 (11) (a) Macatangay, A. V.; Mazzetto, S. E.; Endicott, J. F. *Inorg. Chem.* **1999**, *38*, 5091–5101. (b) Macatangay, A. V.; Endicott, J. F.; Song, X. *J. Phys. Chem. A* **1998**, *39*, 7537–7540. (c) Macatangay, A. V.; Endicott, J. F. *Inorg. Chem.* **2000**, *39*, 437–446.
 (12) Lever, A. B. P. *Inorganic Electronic Spectroscopy*; Elsevier: Amsterdam, 1985.

- (13) Nakamoto, K. *Infrared and Raman Spectra of Inorganic and Coordination Compounds*, 4th ed.; John Wiley & Sons: New York, 1986.
 (14) Bignozzi, C. A.; Argazzi, R.; Schoonover, J. R.; Gordon, K. C.; Dyer, R. B.; Scandola, F. *Inorg. Chem.* **1992**, *31*, 5260–5267.
 (15) (a) Curtis, N. J.; Lawrance, G. A.; Sargeson, A. M. *Inorg. Synth.* **1986**, *24*, 277–279. (b) Lawrance, G. A.; Lay, P. A.; Sargeson, A. M. *Inorg. Synth.* **1986**, *24*, 257–263. (c) Lawrance, G. A.; Sargeson, A. M. *Inorg. Synth.* **1986**, *24*, 250–252.
 (16) Kauffman, G. B.; Teter, L. A. *Inorg. Synth.* **1963**, *7*, 232–236.
 (17) Burewicz, A.; Haim, A. *Inorg. Chem.* **1988**, *27*, 1611–1614.
 (18) Vogler, A.; Osman, A. H.; Kunkely, H. *Inorg. Chem.* **1987**, *26*, 2337–2340.

Table 1. Spectroscopic and Electrochemical Parameters Observed for the Fe–M Dinuclear Mixed-Valence Compounds Synthesized in This Study, along with Their Literature Values (in Parentheses), Where Available^a

M	color	M:Fe ratio	λ_{\max} (nm)	ν_{\max} (kK)	ϵ_{\max} (M ⁻¹ cm ⁻¹)	$\Delta\nu_{1/2}$ (cm ⁻¹)	H_{ab} (cm ⁻¹)	$E_{1/2}^{\text{Fe}}$ (V vs SSE)	$E_{1/2}^{\text{M}}$ (V vs SSE)	$\nu(\text{CN})$ (cm ⁻¹)
Ru	green (green)	0.95 (1.00)	965 (965)	10.4 (10.4)	3100 (3000)	4700 (4900)	1600 (1600)	0.38 (0.42)	-0.33 (-0.28)	2056 (2060)
Os	blue (blue)	0.92 (1.00)	622 (628)	16.1 (15.9)	3100 (3600)	4300 (4300)	1900 (2000)	0.45 ^b	-1.08	2040 (2050)
Cr	yellow-orange	1.00 (1.00)	374 (376)	26.7 (26.6)	2700 (2400)	4800 (6300)	2400 (2600)	0.37	none obsd	2047
Pt	red-orange	1.10 (1.00)	423 (421)	23.7 (23.8)	1000 (540)	7400 (7800)	1700 (1300)	0.56 (0.58)	none obsd	2118, 2054 (2119, 2054)

^a The abbreviations have been defined in the text. H_{ab} was calculated using eq 2, taking 5.0 Å as an estimate of the internuclear separation. All values are the average of those for two to six samples. ^b The tallest and central of a triplet of DPV peaks.

of $\text{K}_4[\text{Fe}(\text{CN})_6]$ (typically, 0.50–1.00 g) and the appropriate $[\text{M}(\text{NH}_3)_5(\text{OSO}_2\text{CF}_3)](\text{OSO}_2\text{CF}_3)_2$ complex were combined in a 1:1 stoichiometric ratio and heated gently for 10–20 min on a hot plate; the mixture was filtered hot to remove any insoluble impurities, including the mixed-valence ion pair salts; and the resulting filtrates were concentrated by slow evaporation in the dark. $[(\text{NH}_3)_5\text{Pt}^{\text{IV}}\text{NC-Fe}^{\text{II}}(\text{CN})_5]$ was synthesized directly from the literature procedure¹⁹ and concentrated in total darkness by evaporation from a watchglass. The resulting concentrated aqueous solutions were purified on a Bio-Gel P2 size exclusion column, collecting the major band. The purified species were then evaporated to dryness in the dark and characterized by UV/vis, IR, and ICP spectroscopies, as well as by differential pulse or cyclic voltammetry. The solid samples were found to be stable for weeks, while the stability of aqueous solutions of these species varied with the metal and with their exposure to light. The degree of hydration for each of these compounds was undetermined.

Synthesis of the Trinuclear Mixed-Valence Compounds. Ten different cyano-bridged trinuclear compounds of the general form $[(\text{NH}_3)_5\text{M-NC-Fe}^{\text{II}}(\text{CN})_4\text{-CN-M}'(\text{NH}_3)_5]^{n+}$ were synthesized for each of the possible permutations where M and M' = Ru^{III}, Os^{III}, Cr^{III}, or Pt^{IV}. The procedure involved mixing ~10 mM aqueous solutions of one of the four dinuclear (Fe–M) mixed-valence compounds (typically 50–100 mg) with an ~10 mM aqueous solution of a pentaammine-trifluoromethanesulfonato metal complex. The resulting mixtures were heated gently for 15–30 min on a hot plate, filtered to remove any insoluble impurities, and then concentrated in the dark. Each species was purified by passage through a Bio-Gel P2 polyacrylamide column. The appropriate band for collection was determined by UV/vis spectroscopy and differential pulse voltammetry. To guarantee that only a single species had been obtained off the Bio-Gel P2 columns and to ensure the reproducibility of the spectroscopic data, each compound was synthesized between 3 and 6 times, beginning with its mononuclear components. The purified species were then evaporated to dryness in the dark and characterized by UV/vis, IR, and ICP spectroscopies, as well as by differential pulse or cyclic voltammetry. The solid samples were found to be stable for weeks, while the stability of aqueous solutions of these species varied with the metal and with their exposure to light. Aqueous solutions containing M or M' = Cr seemed particularly unstable with respect to ligand substitution, and solutions containing M or M' = Cr or Pt were noticeably light-sensitive. Therefore, both UV/vis spectroscopy and electrochemical measurements were typically performed within 30 min of their elution from the Bio-Gel column. The degree of hydration for each of the solid compounds was undetermined.

Results and Discussion

Synthesis and Purification. The syntheses of the four dinuclear mixed-valence species have been reported previously.^{17–19} While slight modifications to the literature procedures were employed in certain instances, the integrity of each of these compounds was confirmed by a comparison of their spectroscopic properties with those in the chemical literature. Each species contains a broad IT absorption band in the visible or near-IR region of the electromagnetic spectrum. A comparison

of the observed and literature parameters for each of these compounds can be found in Table 1. In all four cases, there is reasonable agreement of the absorption band energies and molar absorptivities with their literature values. Likewise, the half-widths of the IT bands agree well with the literature, with the exception of the Fe–Cr complex. We have evaluated this parameter for five separate Fe–Cr samples with an average deviation of only 200 cm⁻¹, giving us confidence in the present value. In the two instances in which they were reported, the standard reduction potentials for the dinuclear mixed-valence species also correspond well with those reported by the original authors.^{19,20}

The syntheses of the ten M–Fe–M' trinuclear mixed-valence compounds proceeded by a substitution reaction between the dinuclear $[(\text{NH}_3)_5\text{M-NC-Fe}(\text{CN})_5]^{n-}$ mixed-valence species and $[\text{M}(\text{NH}_3)_5(\text{OSO}_2\text{CF}_3)]^{n+}$. This synthetic strategy exploits the well-documented lability of trifluoromethanesulfonato metal complexes that results from a combination of the triflate ion's large electronegativity and the resonance stabilization of its negative charge.²¹ The triflate ion is an excellent leaving group, and the pentaamminetrifluoromethanesulfonato metal complexes rapidly aquate when dissolved in water.¹⁷ Since the N-terminus of the Fe–M cyanometalates can serve as a strong σ donor with an affinity for electron-poor metals, it readily substitutes for the aqua ligand to form the cyano-bridged compounds. Gentle heating was employed to ensure that the reactions proceeded to equilibrium in a reasonable period of time. In the case of each asymmetric complex (M \neq M'), the synthesis of M–Fe–M' was performed successfully by reacting either Fe–M with M' or Fe–M' with M, as determined by UV/vis, ICP, and DPV. Typical yields (after purification) for the trinuclear mixed-valence compounds were between 10 and 40%. In general, the yields were larger when Fe–M contained Ru or Os.

Each species was purified by passage through a Bio-Gel P2 size exclusion polyacrylamide gel. The different fractions from the columns were identified based on UV/vis spectroscopy, electrochemical measurements, and inductively coupled plasma (metal:metal ratios). Undesirable fractions frequently included higher-order species containing more than three metals, unreacted dinuclear compounds, and their mononuclear fragments. On no occasion during the purification of the asymmetric species were any of the corresponding symmetric compounds observed. This implies that the asymmetric mixed-valence compounds are relatively inert with respect to substitution on the time scale necessary to run the chromatography.

Additionally, both cis and trans isomers are possible for the trinuclear species. In a few instances, two bands were eluted from the size exclusion column which both contained evidence for the presence of all three metals. The IT bands for the two

(20) Dong, Y.; Hupp, J. T. *Inorg. Chem.* **1992**, *31*, 3322–3324.

(19) Pfennig, B. W.; Lockard, J. V.; Cohen, J. L.; Watson, D. F.; Ho, D. M.; Bocarsly, A. B. *Inorg. Chem.* **1999**, *38*, 2941–2946.

(21) Dixon, N. E.; Lawrance, G. A.; Lay, P. A.; Sargeson, A. M. *Inorg. Chem.* **1984**, *23*, 2940–2947.

Table 2. Spectroscopic and Electrochemical Parameters Observed for the $M'-Fe-Ru$ Trinuclear Mixed-Valence Compounds Synthesized in This Study, as Well as for the Corresponding Dinuclear Compound $Fe-Ru^a$

M'	color	M:Fe ratio	λ_{max} (nm)	ν_{max} (kK)	ϵ_{max} ($M^{-1} cm^{-1}$)	$\Delta\nu_{1/2}$ (cm^{-1})	H_{ab} (cm^{-1})	$E_{1/2}^{Fe}$ (V vs SSE)	$E_{1/2}^{Ru}$ (V vs SSE)	$\nu(CN)$ (cm^{-1})
none	green	0.95	965	10.4	3100	4700	1600	0.38	-0.33	2056
Ru	teal	2.10	879	11.4	5500	4800	1600	0.55	-0.31, -0.38	2053
Os	blue	0.92	876	11.4	3200	4200	1600	0.62	-0.31	2047
Cr	green	1.07	860	11.6	3000	4300	1600	0.56	-0.31	2056
Pt	brown-green	1.08	808	12.4	2600	4700	1600	0.67	-0.37	2067

^a The abbreviations have been defined in the text. H_{ab} was calculated using eq 2, taking 5.0 Å as an estimate of the internuclear separation and using $g = 2$ for the symmetrical species. All values are the average of those for two to six samples.

Table 3. Spectroscopic and Electrochemical Parameters Observed for the $M'-Fe-Os$ Trinuclear Mixed-Valence Compounds Synthesized in This Study, as Well as for the Corresponding Dinuclear Compound $Fe-Os^a$

M'	color	M:Fe ratio	λ_{max} (nm)	ν_{max} (kK)	ϵ_{max} ($M^{-1} cm^{-1}$)	$\Delta\nu_{1/2}$ (cm^{-1})	H_{ab} (cm^{-1})	$E_{1/2}^{Fe}$ (V vs SSE)	$E_{1/2}^{Os}$ (V vs SSE)	$\nu(CN)$ (cm^{-1})
none	blue	0.95	622	16.1	2300	4300	1600	0.45 ^b	-1.08	2044
Ru	blue	0.94	592	16.9	2000	4600	1600	0.62	-1.10	2047
Os	purple	1.96	580	17.2	6000	4700	2000	0.67	-1.09	2062
Cr	blue	1.12	584	17.1	2800	4100	1800	0.60	-1.09	2054
Pt	red-purple	0.88	566	17.7	2700	4100	1800	0.75	-1.12	2059

^a The abbreviations have been defined in the text. H_{ab} was calculated using eq 2, taking 5.0 Å as an estimate of the internuclear separation and using $g = 2$ for the symmetrical species. All values are the average of those for two to six samples. ^b The tallest and central of a triplet of DPV peaks.

Table 4. Spectroscopic and Electrochemical Parameters Observed for the $M'-Fe-Cr$ Trinuclear Mixed-Valence Compounds Synthesized in This Study, as Well as for the Corresponding Dinuclear Compound $Fe-Cr^a$

M'	color	M:Fe ratio	λ_{max} (nm)	ν_{max} (kK)	ϵ_{max} ($M^{-1} cm^{-1}$)	$\Delta\nu_{1/2}$ (cm^{-1})	H_{ab} (cm^{-1})	$E_{1/2}^{Fe}$ (V vs SSE)	$E_{1/2}^{Cr}$ (V vs SSE)	$\nu(CN)$ (cm^{-1})
none	yellow-orange	1.00	374	26.7	2700	4800	2400	0.37	not obsd	2047
Ru	green	0.82	355	28.1	2600	5200	2500	0.56	not obsd	2056
Os	blue	0.87	360	27.8	6100	5200	3800	0.60	not obsd	2054
Cr	yellow	1.85	361	27.7	5700	5100	2600	0.58	not obsd	2050
Pt	yellow-orange	0.86	346	28.9	2200	4700	2300	0.70	not obsd	2068

^a The abbreviations have been defined in the text. H_{ab} was calculated using eq 2, taking 5.0 Å as an estimate of the internuclear separation and using $g = 2$ for the symmetrical species. All values are the average of those for two to six samples.

Table 5. Spectroscopic and Electrochemical Parameters Observed for the $M'-Fe-Pt$ Trinuclear Mixed-Valence Compounds Synthesized in This Study, as Well as for the Corresponding Dinuclear Compound $Fe-Pt^a$

M'	color	M:Fe ratio	λ_{max} (nm)	ν_{max} (kK)	ϵ_{max} ($M^{-1} cm^{-1}$)	$\Delta\nu_{1/2}$ (cm^{-1})	H_{ab} (cm^{-1})	$E_{1/2}^{Fe}$ (V vs SSE)	$E_{1/2}^{Pt}$ (V vs SSE)	$\nu(CN)$ (cm^{-1})
none	red-orange	1.10	423	23.7	1000	7400	1700	0.56	not obsd	2118, 2054
Ru	brown-green	0.87	400	25.0	1000	6700	1700	0.67	not obsd	2067
Os	red-purple	0.78	413	24.2	3800	10 000	3900	0.75	not obsd	2059
Cr	yellow-orange	1.14	435	23.0	1100	6000	1600	0.70	not obsd	2068
Pt	peach	2.18	399	25.1	1900	7800	1800	0.79	not obsd	2055

^a The abbreviations have been defined in the text. H_{ab} was calculated using eq 2, taking 5.0 Å as an estimate of the internuclear separation and using $g = 2$ for the symmetrical species. All values are the average of those for two to six samples.

fractions and the electrochemical potentials of the metal centers were different for the two species, even though they exhibited similar metal:metal ratios. In these cases, it is not known whether the two fractions consisted of separate geometrical isomers or whether the second band might have been due to a substitution product of one of the other ligands on the terminal metal centers. The reproducibility of the spectroscopic and electrochemical results for the major product which resulted from separate syntheses implies that a single specific geometrical isomer has been obtained in most other cases, since the cis and trans isomers should exhibit slightly different IR spectra, UV/vis spectra, and electrochemistry and it is unlikely that the exact same product distribution was achieved in subsequent syntheses. While IR studies exist of related trinuclear cyano-bridged MV species in which the cis or trans geometry is known, the energies of the IR stretches are often similar and their intensities are not always comparable.^{11a,14} Since only a single broad $\nu(CN)$ is observed for the complexes of interest and its width might easily obscure

any nearby or weaker modes, a definitive geometric assignment cannot be made on the basis of IR evidence. The only known crystal structure of a related cyano-bridged mixed-valence coordination compound is that of $[dmbRe^I(CO)_3(\mu-NC)]_3Fe^{III}(CN)_3$.²² This tetranuclear species has a ferricyanide center with three pendant $dmbRe^I(CO)_3-$ fragments bridged by separate cyanide ligands. The equatorial arrangement of the three Re species around the central Fe unit implies that the trinuclear $Re-Fe-Re$ precursor adopted a trans configuration so as to avoid the large steric interactions evident in the crystal structure between the bulky Re appendages. Certainly, more structural data is necessary in order to confirm whether a trans isomer also predominates in the present trinuclear systems.

Eight of the ten trinuclear $M-Fe-M'$ (M or $M' = Ru, Os, Cr, or Pt$) mixed-valence complexes are novel compounds. The

(22) Pfennig, B. W.; Cohen, J. L.; Sosnowski, I.; Novotny, N. M.; Ho, D. M. *Inorg. Chem.* **1999**, *38*, 606–612.

other two (with $M = M' = \text{Ru}$ or Os) have been synthesized previously by inner-sphere cluster formation.²³ Attempts by these authors to purify the Ru–Fe–Ru complex using cation ion exchange chromatography yielded two fractions with absorption bands at 872 and 880 nm. The former of these was attributed to incomplete separation of a mixture of geometrical isomers, while the latter was assumed to be a single isomer. The energy of the reported IT band is in close agreement with the value of 879 nm obtained for Ru–Fe–Ru in this study. The electrochemical results for this complex also correspond well with those in the literature. These results will be discussed in further detail in a later section.

Each of the four symmetrical compounds contained a single broad IT band in the visible or near-IR, while the six asymmetric trinuclear compounds exhibited two IT absorptions. The assignments of these bands are listed in Tables 2–5 and are based on a comparison of their energies to those of the corresponding dinuclear mixed-valence compounds. The spectroscopic and electrochemical data for the trinuclear compounds are organized into four separate tables so that a direct comparison of specific $\text{Fe} \rightarrow \text{M}$ IT band parameters can be drawn across each series as M' is varied. These parameters can likewise be related to those of the corresponding dinuclear species, which is also listed in each table. For example, while two separate IT bands occur in Ru–Fe–Os, those properties relating to the $\text{Fe(II)} \rightarrow \text{Ru(III)}$ IT band are found in Table 2 and can be compared with the $\text{Fe(II)} \rightarrow \text{Ru(III)}$ IT band parameters for Fe–Ru, Ru–Fe–Ru, Cr–Fe–Ru, and Pt–Fe–Ru, while the IT band properties relating to the $\text{Fe(II)} \rightarrow \text{Os(III)}$ band in Ru–Fe–Os are listed in Table 3. It should be noted that, in actuality, all of these compounds exist within strongly coupled supramolecular complexes and that the possibility of mixing between the three metal centers through the bridging cyanides might therefore preclude such simplistic assignments. Thus, for example, the assignments of the 592 and 876 nm absorptions in Ru–Fe–Os should be more properly considered as *predominantly* $\text{Fe(II)} \rightarrow \text{Os(III)}$ and $\text{Fe(II)} \rightarrow \text{Ru(III)}$ intervalent transitions, respectively. The higher energy IT bands might also contain a significant bridging ligand contribution from mixing with the MLCT and/or LMCT transitions which occur in the UV and near-UV. Indeed, Scandola has postulated that electronic coupling can occur in cyano-bridged mixed-valence compounds through a superexchange mechanism involving high-energy charge transfer states associated with the bridging ligand.⁹

Electrochemical Studies. The half-wave potentials of the mixed-valence species reported in Tables 1–5 were measured in 0.2 M KNO_3 solutions by either cyclic or differential pulse voltammetry using a carbon button working electrode, a platinum counter, and an SSE reference. Potassium ferricyanide was used to ensure proper calibration of the reference electrode between experiments. Most of the trinuclear compounds yielded poor cyclic voltammograms as a result of the low concentrations of these complexes, and DPV was therefore found to be a more informative technique. The baseline-corrected DPV for Os–Fe–Ru is shown in Figure 1(top), while that of Ru–Fe–Ru appears in Figure 1 (bottom). For those compounds for which CV could be performed, the redox waves were quasi-reversible, exhibiting peak-to-peak separations which were scan-rate dependent and larger than the 59 mV expected for electrochemically reversible systems.

The half-wave potential observed for the Fe(II/II) couple in the differential pulse voltammograms of each dinuclear MV

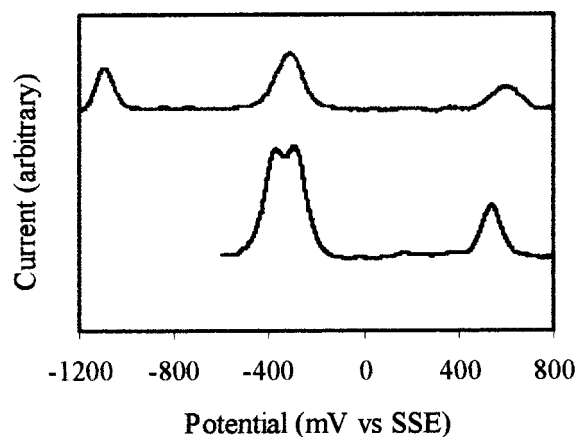


Figure 1. Baseline-corrected differential pulse voltammogram for Os–Fe–Ru (top) and Ru–Fe–Ru (bottom) in 0.2 M KNO_3 using a C/Pt/SSE electrode system and a scan rate of 4 mV/s, an amplitude of 10 mV, and a 50 ms pulse width.

compound was shifted to more positive potentials than that observed for potassium ferricyanide (0.23 V), ranging from 0.37 V for Fe–Cr to 0.56 V for Fe–Pt (Table 1). This shift is characteristic of the removal of electron density from the Fe(II) center by formation of a coordinate covalent bond between the N-terminus of the cyanide bridge and the acceptor metal and has been observed for a large number of compounds.^{17,19,23,24} The magnitude of the electrochemical shift depends both on the electrophilicity of M and the degree of electronic coupling in the D/A complex. For the Fe–Ru and Fe–Os compounds, a second redox event occurred at significantly more negative potentials and was assigned to the Ru(III/II) and Os(III/II) couples, respectively. The Cr and Pt moieties in Fe–Cr and Fe–Pt were electrochemically silent as a result of the slow charge-transfer kinetics associated with their larger reorganization energies.

Each of the ten trinuclear $M\text{--Fe--}M'$ mixed-valence compounds exhibited a DPV peak between 0.55 and 0.80 V vs SSE which could be attributed to the Fe(III/II) couple. In every instance, the Fe wave was shifted more positive than that for the dinuclear species by several hundred millivolts. This additional positive shift reflects the further withdrawal of electron density from the Fe(II) center as a result of the second acceptor metal coordinating to the central Fe through a cyanide bridge. Several multinuclear mixed-valence species in the chemical literature, such as Fe--Pt_n ²⁵ and Fe--Re_n ²² ($n = 1\text{--}3$), have demonstrated nearly monotonic increases in $E_{1/2}$ for the central iron moiety as the value of n increases. The additive nature of the two terminal metals on $E_{1/2}(\text{Fe})$ in the mixed-valence systems in this work was less definitive. Nonetheless, across each series of $M\text{--Fe--}M'$ compounds listed in Tables 2–5 where M was held constant as M' was varied, $E_{1/2}(\text{Fe})$ increased in the order $M' = \text{Cr} \sim \text{Ru} < \text{Os} < \text{Pt}$. It is no coincidence that this is the same order in which $E_{1/2}(\text{Fe})$ increased across the dinuclear series (Table 1).

No redox events were observed for the Cr or Pt couples in the differential pulse voltammograms for the trinuclear species. For those complexes containing Ru or Os, half-wave potentials attributable to these metals were observed (Tables 2 and 3).

(23) Pouloupoulou, V. G.; Taube, H.; Nunes, F. S. *Inorg. Chem.* **1999**, *38*, 2844–2850.

(24) (a) Zhou, M.; Pfennig, B. W.; Steiger, J.; Van Engen, D.; Bocarsly, A. B. *Inorg. Chem.* **1990**, *29*, 2456–2460. (b) Pfennig, B. W.; Bocarsly, A. B. *J. Phys. Chem.* **1992**, *96*, 226–233. (c) Wu, Y.; Cochran, C.; Bocarsly, A. B. *Inorg. Chim. Acta* **1994**, *226*, 251–258. (d) Pfennig, B. W.; Goertz, J. K.; Wolff, D. W.; Cohen, J. L. *Inorg. Chem.* **1998**, *37*, 2608–2611.

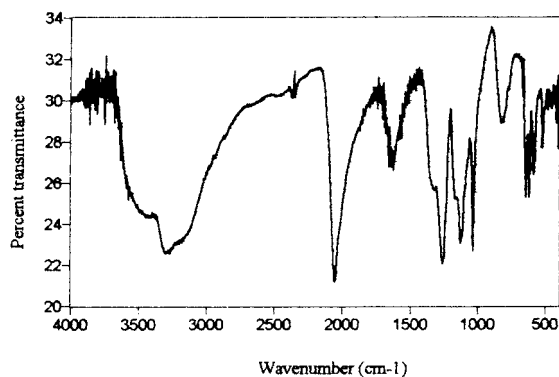


Figure 2. IR spectrum (KBr pellet) of Os–Fe–Ru from 4000 to 400 cm^{-1} with a resolution of 2 cm^{-1} .

Throughout both series, the potential of Ru or Os (where $M' = \text{Ru, Os, or Cr}$) agreed within 20 mV to that in the dinuclear compounds. For $M' = \text{Pt}$, $E_{1/2}$ for Ru and Os in Pt–Fe–Ru and Pt–Fe–Os, respectively, was shifted 40 mV to more negative potentials than that of the corresponding dinuclear species. This increased difference is probably a result of the larger positive charge on the supramolecular complexes when Pt(IV) replaces Ru(III), Os(III), or Cr(III). As a general rule, however, the Ru and Os half-wave potentials in the trinuclear species differed only slightly from those in the corresponding dinuclear complexes. It can therefore be concluded that, in most cases, the electronic distributions in the terminal metals are relatively unaffected by the presence of the third metal. One notable exception is the observation of two distinct redox events attributable to Ru in Ru–Fe–Ru (Table 2, Figure 1, bottom). While this result might be interpreted in terms of the possibility that these waves correspond to the presence of both cis and trans isomers which contain Ru in slightly different environments, the equal peak heights for the two waves and the reproducibility of these relative peak heights in samples resulting from different syntheses imply that this explanation might be an oversimplification. The possibility that the two redox waves occur as a result of remote electronic coupling will be considered in a later section.

Infrared Spectroscopy. The IR spectra of each trinuclear compound exhibit peaks corresponding to each pentaammine metal moiety, the central ferrocyanide, and the triflate anions. The IR spectrum of Os–Fe–Ru is shown in Figure 2 as a representative example. Based on comparisons with the mononuclear components or their nearest approximations,¹³ the following tentative assignments have been made for the IR peaks in Os–Fe–Ru: 3573, 3271 cm^{-1} ($\nu_{\text{as}}(\text{NH})$); 2047 cm^{-1} ($\nu(\text{CN})$); 1621 cm^{-1} ($\delta_{\text{a}}(\text{NH}_3)$); 1295 cm^{-1} ($\delta_{\text{s}}(\text{NH}_3)$); 1254, 1123, 1026 cm^{-1} ($\nu_{\text{as}}(\text{OSO})$, triflate anion); 821, 810 cm^{-1} ($\rho_{\text{r}}(\text{NH}_3)$); 640, 620 cm^{-1} ($\nu(\text{FeC})_{\text{b}}$); 578 cm^{-1} ($\nu(\text{FeC})_{\text{t}}$); 516 cm^{-1} ($\nu(\text{RuN})$); and 419 cm^{-1} ($\nu(\text{OsN})$). Despite the low symmetry of the trinuclear complexes and the presence of several kinds of terminal and bridging cyanide ligands, only a single broad $\nu(\text{CN})$ was observed in the IR spectra of the 10 trinuclear mixed-valence compounds (Tables 1–5). The number and energies of $\nu(\text{CN})$ stretches in cyano-bridged D/A complexes depends on several contributing factors:^{8,13,14} (1) the oxidation state of the metal, (2) symmetry considerations, (3) kinematic coupling of the bridging cyanide caused by its constraint between two heavy metal centers, (4) the degree of π back-bonding between the metal and either terminus of the bridging cyanide, and (5) the degree of electronic coupling between the donor and acceptor metals. The energy of the single $\nu(\text{CN})$ vibrational frequency varied over a surprisingly small range (2047–2068 cm^{-1}),

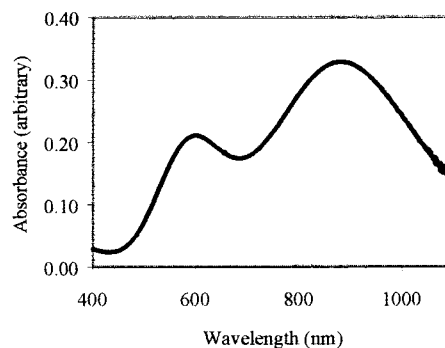


Figure 3. Electronic absorption spectrum of Os–Fe–Ru from 300 to 1100 nm in aqueous solution using distilled water as the reference spectrum.

considering the differing degrees of π back-bonding and kinematic coupling expected as M and M' are varied across the series. Each of the $\nu(\text{CN})$ frequencies was much closer in energy to $\nu(\text{CN})$ for $\text{K}_4[\text{Fe}(\text{CN})_6] \cdot 3\text{H}_2\text{O}$ (2044 cm^{-1}) than for $\text{K}_3[\text{Fe}(\text{CN})_6]$ (2118 cm^{-1}),¹³ confirming the formal 2+ oxidation state of iron in each of these compounds.

While dinuclear cyano-bridged mixed-valence compounds, such as $[(\text{NC})_5\text{Fe}^{\text{II}}-\text{CN}-\text{Pt}^{\text{IV}}(\text{NH}_3)_5]$ ¹⁹ and $[(\text{NC})_5\text{Fe}^{\text{II}}-\text{CN}-\text{Co}^{\text{III}}\text{L}]^-$ ($\text{L} = \text{pentadentate macrocyclic amine}$),²⁶ exhibit bridging $\nu(\text{CN})$ stretches which are considerably blue-shifted from their parent cyanometalate, consistent with a kinematic effect, many others are significantly red-shifted.^{8,11} In fact, one study has found that the magnitude of this red shift can be correlated with the oscillator strength of the IT band and therefore with the degree of electronic coupling between the two metals.⁸ The electronic coupling in the Fe–Co and Fe–Pt compounds mentioned above are, for example, smaller than for Fe–Ru, Ru–Ru, or Os–Ru mixed-valence dimers. A vibronic coupling mechanism^{8,11} has been used to explain the bathochromic shifts in $\nu(\text{CN})_{\text{br}}$ for strongly coupled cyano-bridged D/A compounds. According to this model, the bridging ligand's nuclear coordinates are entangled (in equilibrium) with the electronic coordinates. As a result, the CN^- stretching vibration encounters a decreased repulsion with the d_{7z} electrons on the two metals and this leads to a weaker CN^- stretching force constant. The observation of a single broad $\nu(\text{CN})$ at comparatively intermediate energies for the compounds in this study might therefore be a result of the inability to resolve the terminal and bridging cyanide stretches in differing environments or a complex vibronic coupling mechanism involving the $M-\text{NC}-\text{Fe}-\text{CN}-M'$ multicenter.

Electronic Absorption Spectroscopy. Each of the four symmetric trinuclear mixed-valence compounds exhibits a single broad IT absorption in their electronic spectroscopy, while the six asymmetric species display two IT absorptions. In most cases, the IT bands are separated enough in energy that they can be analyzed directly. For those few complexes where the two IT bands overlapped significantly, the spectroscopic parameters listed in Tables 2–5 were obtained by fitting the relevant portion of the electronic spectrum to two overlapping Gaussian transitions. Figure 3 shows the electronic absorption spectrum of Os–Fe–Ru as a representative example. As a general rule, each of the intervalent absorptions is blue-shifted from those of the corresponding dinuclear species. Because the inner-sphere coordination environments of the dinuclear and trinuclear metal complexes are essentially the same, the hyp-

(25) Pfennig, B. W.; Bocarsly, A. B. *Inorg. Chem.* **1991**, *30*, 666–672.

(26) Bernhardt, P. V.; Martinez, M. *Inorg. Chem.* **1999**, *38*, 424–425.

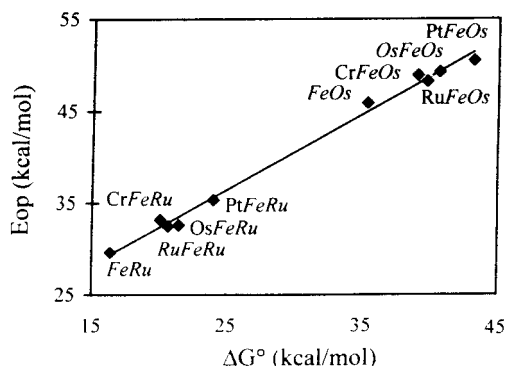


Figure 4. Graph of E_{op} (kcal/mol) vs ΔG° (kcal/mol) for the ten IT bands for which $\Delta E_{1/2}$ can be measured, demonstrating the linear relationship predicted by eq 1. The elements in italics indicate the specific donor and acceptor within each A–D–A' species which are represented by that point.

sochromic shift must result either from the larger D/A $\Delta E_{1/2}$ in the trinuclear compounds or from the outer-sphere reorganization term. The former explanation is consistent with the electrochemical results mentioned above, where the potential of the Fe center shifts more positive with each additional pendant metal while the potential of the terminal metal complexes is largely unaffected.

Equation 1 predicts that the energies of the IT bands for the MV compounds should vary linearly as a function of the thermodynamic driving force, assuming that the reorganization energy is a constant. For those cases where the redox potential of both the donor and acceptor metal can be measured, ΔG° could be calculated from the electrochemical data. Figure 4 depicts a plot of the IT band energy (converted into kcal/mol) vs ΔG° (kcal/mol) for those compounds in Tables 2–5 where $\Delta E_{1/2}$ could be determined. Despite the slightly different reorganization energies expected on the basis of the different metal coordination spheres, the different charges on the MV ions, and the fact that both dinuclear and trinuclear compounds are directly compared, the linear relationship expected by electron transfer theory was nonetheless observed. The slope of this linear fit is 0.82. A slope of 1.00 would be expected only if all of the following were true: (1) the nuclear geometry did not change significantly with the oxidation state, (2) the solvational energies for the ground state and excited state were comparable, (3) there was no significant entropy difference between the two states, and (4) the energy of the IT transition could be estimated as the energy difference between the HOMO and LUMO.²⁷

While the energies of the IT bands in the trinuclear compounds were shifted from their dinuclear analogues, the values of the molar absorptivities and half-widths (properties related to the oscillator strength of the electronic transition) varied from compound to compound. The oscillator strengths of the IT band in the four symmetrical trinuclear mixed-valence compounds were roughly twice the size of those observed for the corresponding dinuclear species. This observation is consistent with Parker and Crosby's prediction for trans A–D–A complexes with degenerate acceptors of a single IT transition with twice the intensity of an individual oscillator.²⁸ The cis geometrical isomer, on the other hand, would be expected to

yield two closely spaced IT bands of comparable intensity. While not all the IT bands could be fit perfectly to a Gaussian band shape, there was no obvious evidence for the presence of multiple transitions under a single absorption band in any of the ten trinuclear compounds. The absence of two IT bands cannot be taken as proof of the trans geometry, however, since their observation in the cis depends on the magnitude of the matrix element which mixes them. In the absence of supporting crystallographic data, therefore, the hypothesized trans geometry of these species could not be confirmed. However, the cleanness of the UV/vis, IR, and electrochemical data strongly suggest the presence of a single isomer.

For the asymmetric Ru series (Table 2), the molar absorptivities and half-widths of the Fe(II) → Ru(III) IT band were roughly comparable with those for the Fe–Ru dinuclear species, given the margin of experimental error (estimated as average deviations of $\pm 350 \text{ M}^{-1} \text{ cm}^{-1}$ and $\pm 250 \text{ cm}^{-1}$, respectively). For the asymmetrical Os, Cr, and Pt series, however, the oscillator strengths of the Fe(II) → Os(III) IT band varied over a wider range. In particular, the intensity of the Fe(II) → Cr(III) and Fe(II) → Pt(IV) IT bands when $M' = \text{Os}$ were noticeably larger than those for the dinuclear species. This result suggests that an intensity-borrowing mechanism might be occurring, whereby the Fe → M IT band borrows intensity from the nearby Fe → Os transition. A less likely explanation is that a solvent effect occurs for these two compounds which contributes to the larger area of the absorption band. In such a case, the outer-sphere reorganization energy should also differ significantly for these species. If this were true, the linear relationship in Figure 4 would be expected to show significant deviations for these two compounds, which it clearly does not. We therefore propose that the observed oscillator strength enhancement can be attributed to an intensity-stealing mechanism.

Intensity stealing can occur when two or more excited states of similar energy and appropriate symmetry mix with each other, where the magnitude of the mixing is proportional to the degree of their orbital overlap. In the asymmetric MV compounds of interest, two IT excited states can be formed depending on the wavelength of light absorbed: $[\text{M}(\text{red})\text{--Fe(III)}\text{--M}'(\text{ox})]^*$ and $[\text{M}(\text{ox})\text{--Fe(III)}\text{--M}'(\text{red})]^*$ (ox = the higher oxidation state of the redox couple and red = the lower oxidation state). If these two excited states mix with each other across the cyanometalate bridge, then one of the IT transitions can steal intensity at the expense of the other. In the case of Os(III)–Fe(II)–M(ox), where M = Cr or Pt, the Fe(II) → M(ox) IT band intensity is significantly enhanced with respect to that for the corresponding dinuclear species (it is also slightly enhanced for M = Ru). At the same time, the oscillator strength of the Fe(II) → Os(III) IT band is somewhat diminished compared to that for a single oscillator in Os(III)–Fe(II)–Os(III), which is assumed to have the same molecular geometry as Os(III)–Fe(II)–M(ox). Thus, it is entirely possible that the Fe → M IT band steals intensity from the Fe → Os one. However, the relative magnitudes of this intensity stealing are not comparable: the oscillator strength of the former band is significantly more enhanced than that of the latter is decreased. It is therefore possible that both IT states are mixed (to unequal extents) with higher lying charge transfer excited states involving the bridging ligand. This might explain why the Fe(II) → M(ox) IT bands for M = Cr and Pt are more enhanced than for M = Ru. The Fe(II) → Cr(III) and Fe(II) → Pt(IV) IT bands lie at higher energy than the Fe(II) → Ru(III) IT band and are therefore at more appropriate energies for

(27) In the absence of a configurational interaction, the optical energy for a singlet to singlet transition is given by $E_{op} = E_{LUMO} - E_{HOMO} - J_{HL} + 2K_{HL}$, where J_{HL} and K_{HL} are the Coulombic and exchange interelectronic interaction integrals. See, for instance: Lever, A. B. P.; Dodsworth, E. S. In *Inorganic Electronic Structure and Spectroscopy*; Solomon, E. I., Lever, A. B. P., Eds.; John Wiley & Sons: New York, 1999; Vol. II, pp 227–289.

(28) (a) Parker, W. L.; Crosby, G. A. *Int. J. Quantum Chem.* **1991**, *39*, 299–308.

mixing with the charge transfer excited states of the bridging ligand, which occur in the UV or near-UV.¹² While a second spectroscopic signature of intensity stealing involves shifts in the energies of the coupled electronic states, the energies of the IT bands in the compounds of interest are already shifted as a function of ΔG° , are extremely broad, and occasionally overlap with each other, making it difficult to confirm this hypothesis.

The observation that the proposed intensity-borrowing mechanism only occurs in those cases where $M' = \text{Os}$ is somewhat perplexing. One possible explanation is the larger orbital size and tendency for Os(II) to undergo strong π back-bonding relative to the other metals. The greater tendency for Os(II) \rightarrow N π back-bonding in $[\text{M}(\text{NH}_3)_5\text{pz}]^{2+}$ (pz = pyrazine) relative to Ru(II) has been used to explain the ~ 5 pH unit shift in $\text{p}K_a$ values for the protonation of these compounds.²⁹ Likewise, the energy of the $\nu(\text{M}-\text{NC})$ stretch in the resonance Raman spectroscopy of cyano-bridged MV compounds is larger for M = Os than for M = Ru, despite its larger molar mass.^{30,31} This indicates a stronger M–N force constant for Os than for Ru and implies some degree of π back-bonding to the bridging cyanide ligand in the Os case. Any Os(II) \rightarrow N π back-bonding which might occur in the $[\text{M}(\text{ox})-\text{Fe}(\text{III})-\text{Os}(\text{II})]^*$ excited state can help to facilitate mixing between this and the $[\text{M}(\text{red})-\text{Fe}(\text{III})-\text{Os}(\text{III})]^*$ excited state, where the excited-state coupling between the remote metal centers is mediated through the intervening cyanometalate bridge.

The Magnitude of the Electronic Coupling, H_{ab} . The values of H_{ab} which are tabulated in Tables 1–5 were calculated using eq 2, where r_{ab} was approximated as 5.0 Å for all of the compounds in this study. This value of r_{ab} was based on the geometric separation between metals in the single-crystal X-ray structures of $\text{Fe}^{\text{II}}-\text{Pt}^{\text{IV}}$ and $\text{Fe}^{\text{II}}-\text{Co}^{\text{III}}$ and will vary slightly with the radius of the $[\text{M}(\text{NH}_3)_5-\text{NC}]$ fragment. There has been considerable evidence in the chemical literature which suggests that for strongly coupled systems (all other things being equal), the value of H_{ab} calculated using eq 2 represents only a lower limit to the actual degree of electronic coupling between the two metal centers. Evidence supporting this assertion derives from faster than predicted back electron transfer rates,³² larger than expected shifts in the $E_{1/2}$'s of the coupled metal centers,³³ a unique shift of the bridging CN[−] IR stretch to lower energies in D/A compounds,⁸ and electroabsorption studies.^{30,31} In fact, Stark spectroscopy performed on Fe–Ru indicates that an upward correction of $\sim 50\%$ for the value of H_{ab} calculated using oscillator strengths is necessary to justify the experimental data.³⁰ Delocalization of the donor metal's electron density through π back-bonding onto the bridging cyanide effectively decreases the actual distance the electron must traverse (r_{ab}), making the crystallographic distance an overestimation. The values of H_{ab} calculated by eq 2 depend on a number of other factors, including the difference in the ground-state D/A orbitals, the extent of mixing of ligand-based excited states with the two electron transfer states (superexchange coupling), and a vibronic coupling model where the nuclear coordinates depend on the amount of charge delocalized onto the bridging ligand. Equation 2 also ignores the possibility that multiple IT transitions might

contribute to the absorption band half-width as a result of the reduced symmetry of these compounds, broadening due to specific solvent interactions, or the presence of spin–orbit coupling. Thus, the calculated values of H_{ab} reported in Tables 1–5 should be considered as only approximate values.

Nonetheless, the relative values of H_{ab} for the Fe \rightarrow M IT bands of Os–Fe–Cr and Os–Fe–Pt species were significantly larger than those for the corresponding dinuclear species. This increased electronic coupling is expected based on the larger oscillator strengths of these transitions, according to eq 2. As mentioned in the preceding section, intensity stealing can occur if the $[\text{M}(\text{III})-\text{Fe}(\text{III})-\text{Os}(\text{II})]^*$ and $[\text{M}(\text{II})-\text{Fe}(\text{III})-\text{Os}(\text{III})]^*$ excited states are electronically coupled to each other. There has been a precedent for *ground-state* electronic coupling between two of the terminal metals in the electrochemical and spectroscopic data for related trinuclear, cyanometalate-bridged mixed-valence compounds. For example, the compounds $[(\text{NH}_3)_5-\text{Ru}^{\text{II}}-\text{NC}-\text{Ru}^{\text{II}}(\text{py})_4-\text{NC}-\text{Ru}^{\text{III}}(\text{NH}_3)_5]^{7+}$ (py = pyridine), $[\text{py}(\text{NH}_3)_4\text{Ru}^{\text{II}}-\text{NC}-\text{Ru}^{\text{II}}(\text{bpy})_2-\text{CN}-\text{Ru}^{\text{III}}(\text{NH}_3)_4\text{py}]^{5+}$ (bpy = 2,2'-bipyridine), *trans*- $[\text{Cl}(\text{py})_4\text{Ru}^{\text{II}}-\text{NC}-\text{Ru}^{\text{II}}(\text{py})_4-\text{CN}-\text{Ru}^{\text{III}}(\text{py})_4\text{Cl}]^+$, and $[(\text{NH}_3)_5\text{Ru}^{\text{II}}-\text{NC}-\text{M}^{\text{II}}\text{L}_2-\text{CN}-\text{Ru}^{\text{III}}(\text{NH}_3)_5]^{7+}$ (M = Ru or Os, L = bpy or 1,10-phenanthroline) all exhibit two redox waves for the $[\text{Ru}(\text{NH}_3)_5-]$ components.^{9,11c,34} Furthermore, “remote” IT bands with weak intensities have also been observed in several strongly coupled cyanometalate-bridged D/A compounds. Scandola has found that the molar absorptivities of these remote IT bands are roughly correlated with the intensities of nearby IT transitions involving the central metal and argues that the remote IT band steals some intensity from the neighboring charge transfer transition.⁹

The observation of “remote” electronic coupling between terminal metals in related cyanometalate-bridged mixed-valence species also merits a reevaluation of the ground-state electrochemical data for Ru–Fe–Ru. We obtained a single major band (using size exclusion chromatography) with an absorption maximum at 879 nm, an Fe redox wave at 0.55 V vs SSE, and two $[\text{Ru}(\text{NH}_3)_5-]$ redox events at -0.31 and -0.38 V vs SSE. As postulated by Pouloupoulou,²³ an incomplete separation of the cis and trans isomers is one possible explanation for the presence of two separate $[\text{Ru}(\text{NH}_3)_5-]$ waves. Other possibilities include (1) the different electrostatics associated with the 2+ charge of the first reduction versus the 1+ charge of the singly reduced species, (2) different solvation energies associated with the fully oxidized and singly reduced species, (3) delocalization mediated through the “NC–Fe^{II}(CN)₄–CN” bridging ligand, or (4) statistical contributions (estimated at 36 mV at 298 K).³⁵ Given the precedent for remote electronic coupling ($H_{ab} \sim 300 \text{ cm}^{-1}$) in the related trinuclear mixed-valence complex⁹ $[(\text{py})(\text{NH}_3)_4\text{Ru}^{\text{II}}-\text{NC}-\text{Ru}^{\text{II}}(\text{bpy})_2-\text{NC}-\text{Ru}^{\text{III}}(\text{NH}_3)_4(\text{py})]^{5+}$, it is entirely feasible that the presence of two distinct $[\text{Ru}(\text{NH}_3)_5-]$ waves separated by 70 mV in the present Ru–Fe–Ru complex is at least partly due to electronic coupling between the remote Ru centers mediated through the ferrocyanide bridging ligand. A more detailed investigation of this hypothesis will serve as the focus of a future manuscript.

Conclusions

The role of the bridging ligand in promoting electronic coupling between adjacent metal centers is an issue of fundamental importance to electron transfer research. Cyano-bridged mixed-valence compounds represent ideal systems for the study

(29) Taube, H. *Pure Appl. Chem.* **1979**, *51*, 901.

(30) Doorn, S. K.; Blackburn, R. L.; Johnson, C. S.; Hupp, J. T. *Electrochim. Acta* **1991**, *36*, 1775–1785.

(31) Doorn, S. K.; Hupp, J. T. *J. Am. Chem. Soc.* **1989**, *111*, 1142–1144.

(32) Buranda, T.; Lei, Y.; Endicott, J. F. *J. Am. Chem. Soc.* **1992**, *114*, 6917–6919.

(33) Endicott, J. F.; Song, X.; Watzky, M. A.; Buranda, T.; Lei, Y. *Chem. Phys.* **1993**, *176*, 427–438.

(34) Coe, B. J.; Meyer, T. J.; White, P. S. *Inorg. Chem.* **1995**, *34*, 3600–3609.

(35) Goldsby, K. A.; Meyer, T. J. *Inorg. Chem.* **1984**, *23*, 3002–3010.

of electronic coupling as a result of the short length and unique electronic properties of the cyanide ligand. The trinuclear compounds in this work are of the general type A–D–A', where D represents not only the electron donor, but also a supramolecular "NC–Fe^{II}(CN)₄–CN" ligand bridge. The goal of this study was to discover how the electronic coupling between a D/A pair could be influenced by the presence of a second adjacent acceptor. In most of the compounds studied, there were no noticeable differences between the spectroscopic parameters relevant to the electron transfer process in the trinuclear species from those of their dinuclear counterparts. In these cases, the A–D–A' compounds could essentially be considered as back-to-back dinuclear MV compounds which happened to share the same central metal. However, those complexes with M' = Os exhibited significantly enhanced Fe/M electronic coupling which seemed to result uniquely from the presence of the attached Os(III) group. One possible explanation for the spectroscopic observations is that intensity stealing occurs as a result of mixing

of the [Os(II)–Fe(III)–M(ox)]* and [Os(III)–Fe(III)–M(red)]* intervalent excited states with each other and with higher lying charge transfer states involving the bridging ligand. This mixing would be facilitated by the large orbital size of Os(II) and its ability to undergo strong π back-bonding with the cyanometalate bridging ligand in the excited state. Lastly, the two separate redox waves for the geometrically equivalent Ru groups in Ru–Fe–Ru were proposed to result in part from a ground-state mixing of these remote metal centers mediated through the ferrocyanide ligand bridge.

Acknowledgment. The authors acknowledge E. Stout and J. Cohen for experimental assistance and A. Bocarsly for the donation of chloroplatinic acid. B.W.P. is grateful for the support of the Camille & Henry Dreyfus Foundation in the form of a faculty start-up grant and the Research Committee at Vassar College for additional financial support of this project.

IC000706U